Effects of increasing hydrophobicity on the physical-chemical and biological properties of a class A amphipathic helical peptide

Geeta Datta,* Manjula Chaddha,* Susan Hama,† Mohamad Navab,† Alan M. Fogelman,† David W. Garber,* Vinod K. Mishra,* Richard M. Epand,§ Raquel F. Epand,§ Sissel Lund-Katz, Michael C. Phillips,** Jere P. Segrest,* and G. M. Anantharamaiah[1,*]**

The Atherosclerosis Research Unit and the Departments of Medicine and Biochemistry and Molecular Genetics,* The University of Alabama at Birmingham Medical Center, Birmingham, AL 35294; The Atherosclerosis Research Unit,† UCLA Cardiology, Los Angeles, CA 90095; Department of Biochemistry,§ McMaster University, Health Sciences Center, Hamilton, Ontario, Canada L8N 3Z5; and Stokes Research Institute,** Children's Hospital of Philadelphia, Philadelphia, PA 19104

Abstract **We have recently shown that a class A amphipathic peptide 5F with increased amphipathicity protected mice from diet-induced atherosclerosis (Garber et al. *J. Lipid Res.* 2001. 42: 545–552). We have now examined the effects of increasing the hydrophobicity of a series of homologous class A amphipathic peptides, including 5F, on physical and functional properties related to atherosclerosis inhibition by systematically replacing existing nonpolar amino acids with phenylalanine. The peptides, based on the sequence Ac-D-W-L-K-A-F-Y-D-K-V-A-E-K-L-K-E-A-F-NH_2 (Ac-18A-NH_2 or 2F) were: 3F[3](Ac-F[3]18A-NH_2), 3F[14](Ac-F[14]18A-NH_2), 4F(Ac-F[3,14]18A-NH_2), 5F(Ac-F[11,14,17] 18A-NH_2), 6F(Ac-F[10,11,14,17]18A-NH_2), and 7F(Ac-F[3,10,11,14,17] 18A-NH_2). Measurements of aqueous solubility, HPLC retention time, exclusion pressure for penetration into an egg phosphatidylcholine (EPC) monolayer, and rates of EPC solubilization revealed an abrupt increase in the hydrophobicity between peptides 4F and 5F; this was accompanied by increased ability to associate with phospholipids. The peptides 6F and 7F were less effective, indicating a limit to increased hydrophobicity for promoting lipid interaction in these peptides. Despite this marked increase in lipid affinity, these peptides were less effective than apoA-I in activating the plasma enzyme, lecithin:cholesterol acyltransferase, with 5F activating LCAT the best (80% of apoA-I). Peptides 4F, 5F, and 6F were equally potent in inhibiting LDL-induced monocyte chemotactic activity.** **These studies suggest that an appropriate balance between peptide-peptide and peptide-lipid interactions is required for optimal biological activity of amphipathic peptides. These studies provide a rationale for the design of small apoA-I-mimetics with increased potency for atherosclerosis inhibition.**—Datta, G., M. Chaddha, S. Hama, M. Navab, A. M. Fogelman, D. W. Garber, V. K. Mishra, R. M. Epand, R. F. Epand, S. Lund-Katz, M. C. Phillips, J. P. Segrest, and G. M. Anantharamaiah. **Effects of increasing hydrophobicity on the physical-chemical and biological properties of a class A amphipathic helical peptide. *J. Lipid Res.* 2001. 42: 1096–1104.**

Supplementary key words amphipathic α-helix • apoA-I analogs • hydrophobicity • LCAT • synthetic peptides • monocyte chemotactic activity

Plasma levels of high density lipoproteins and apolipoprotein A-I (apoA-I), the major protein constituent of HDL, are inversely correlated to coronary artery disease (CAD) (1, 2). Human apoA-I is a 243 residue protein, containing eight 22-mer amphipathic helical repeats, the majority of which have been shown to possess the Class A motif (3, 4). Class A amphipathic helices have a characteristic charge distribution; they have a cluster of positively charged amino acids at the polar/nonpolar boundary of the α helix and negatively charged residues at the center of the polar face (3–5). This unique secondary structural motif has been postulated to be responsible for the lipid-associating property of apoA-I (3). Many studies with synthetic analogs of Class A amphipathic helices have supported this concept (6, 7). Recently, we have synthesized each of the putative 22-mer helices present in human apoA-I as monomers and tandem dimers and shown that the N- and C-terminal amphipathic helices possess the max-

Abbreviations: Ac_2O, acetic anhydride; apoA-I, apolipoprotein A-I; CAD, coronary artery disease; CD, circular dichroism; DiPoPE, Di (16:1) palmitoleoyl phosphatidylethanolamine; DMPC, dimyristoyl phosphatidylcholine; EPC, egg phosphatidylcholine; FMOC, fluorinylmethyloxycarbonyl; Gdn.HCl, guanidine hydrochloride; HAEC, human aortic endothelial cells; HASMC, human aortic smooth muscle cells; HBTU, 2-(H-benzotriazole-1-yl)-1,1,3,3-tetramethyluronium hexafluorophosphate; MCP-1, monocyte chemotactic protein-1; M-CSF, macrophage colony-stimulating factor; MLV multilamellar vesicles; NMM, N-methylmorpholine; RP-HPLC, reverse phase high performance liquid chromatography; TFA, trifloroacetic acid.

[1] To whom correspondence should be addressed.
e-mail: ananth@uab.edu

imum lipid-associating ability (8). X-ray crystal structure and molecular modeling studies of the exon 4 (44–243 residues) of apoA-I suggests that a self-associated state of the entire apoA-I is necessary for lipid association (9, 10). In this model, two molecules of apoA-I are arranged in the form of a head-to-tail dimer with the monomers interacting with each other to stabilize the lipid-associated structure of apoA-I (11).

Experimental evidence suggests that the protective effect of apoA-I and HDL against coronary artery disease could be due to their role in "reverse cholesterol transport" (12, 13). Reverse cholesterol transport is the sum of three steps involving HDL/apoA-I: *a)* efflux of cholesterol from peripheral cells (14, 15), *b)* esterification by lecithin:cholesterol acyltransferase of HDL-associated cholesterol (16, 17), and *c)* receptor-mediated delivery of cholesterol ester to the liver (18). In vivo studies have shown that both human apoA-I and a class A synthetic amphipathic helical peptide inhibit atherosclerosis without altering plasma cholesterol levels by a mechanism that is independent of reverse cholesterol transport (19, 20). Recently, inhibition of LDL-induced monocyte chemotaxis into artery wall cells has been suggested to be another major role played by apoA-I and HDL in preventing atherosclerosis (20–22).

A peptide that has been shown to mimic the properties of human apoA-I, 18A, has also been shown to possess LCAT activating (23, 24) and cholesterol effluxing abilities (25, 26). Neutralizing the terminal charges of 18A to form Ac-18A-NH_2 was shown to increase its lipid affinity and biological activities (26, 27). Several modifications of the amino acid sequence of this "parent" molecule, 18A, have been made in an attempt to improve its apoA-I-mimicking properties (7, 28, 29). Our earlier studies (7, 24) have shown that an increase in the hydrophobicity of this peptide increases its lipid affinity and apoA-I-mimicking properties. A synthetic peptide 5F, an analog of Ac-18A-NH_2 with increased amphipathicity, has been shown to inhibit diet-induced atherosclerosis in mice (20). However, the peptide 2F did not significantly inhibit diet-induced lesion formation in C57 BL6 mice (30). A study of 18A dimer peptides indicated that increased peptide-peptide association decreased peptide: lipid association (29). To determine the maximum extent to which the lipid affinity of the 18A peptide can be increased with a positive effect on lipid-associating and apoA-I-mimicking properties, we designed a homologous series of peptides in which Phe residues were systematically increased by substituting hydrophobic amino acids such as Leu and Ala on the nonpolar face with Phe. According to the experimentally determined hydrophobicity scale of Wimley and White (31), Trp and Phe are the most hydrophobic amino acids in the sense that they exhibit the greatest partitioning into the membrane from the aqueous phase. We elected to use Phe to increase the hydrophobicity of the peptide because it is the most acid-resistant hydrophobic amino acid in membrane active peptides and Phe-containing peptides can be synthesized more easily than Trp-containing peptides. The effects of this increase in hydrophobicity on the physical and lipid associating properties, and apoA-I-mimicking biological properties such as LCAT activation and inhibition of LDL-induced chemotactic activities, were studied.

EXPERIMENTAL PROCEDURES

Peptide synthesis

The peptides were synthesized by the solid phase method using an automated solid phase synthesizer (PS3 Protein Technologies, Woburn, MA). Fluorinylmethyloxycarbonyl (FMOC)-amino acids were coupled to a rink amide resin (0.536 mEq/g) (Peninsula Laboratories, Inc., Belmont, CA) in the presence of 2-(H-benzotriazole-1-yl)-1,1,3,3-tetramethyluronium hexafluorophosphate (HBTU) and N-methylmorpholine (NMM), and acetylated with acetic anhydride at the N-terminus. The peptides were cleaved from the solid support using 70% TFA in dichloromethane in presence of anisole (1%), mercaptoeathanol (0.1%), and tryptophan (20% by weight of the peptide resin), and purified on a VYDAC C-4 (22 mm × 25 cm, particle size 10 μm) reverse phase high performance liquid chromatography (RP-HPLC) column using a gradient of 25% to 58% acetonitrile in water containing 0.1% trifloroacetic acid (TFA) in 66 min with a flow rate of 4.8 ml/min. The purity of the peptides was verified by analytical RP-HPLC using a C_{18} column (VYDAC, 4.6 mm × 25 cm, 5 μm) and a linear acetonitrile-water (in presence of 0.1% TFA) gradient of 25% to 58% in 33 min, and by the mass spectral analysis.

Circular dichroism

Circular dichroism (CD) spectra were recorded on an AVIV 62DS spectropolarimeter as described earlier (28). Briefly, spectra were obtained using a cell with a 0.1 cm path length and measurements were taken every nm from 260 nm to 190 nm at 25°C. All the CD spectra were signal averaged by adding four scans, base line corrected, and smoothed. Peptide solutions in PBS, pH 7.4, were used at a concentration of 11 μM. Peptide-dimyristoyl phosphatidylcholine (DMPC) complexes (1:20 mol:mol) were used to determine the effect of lipid binding on the helicity of these peptides. These complexes were prepared by adding the appropriate volume of peptide solution to DMPC multilamellar vesicles. DMPC multilamellar vesicles were prepared as follows: A known amount of lipid was dissolved in ethanol and the solvent was removed by evaporating slowly under a thin stream of nitrogen. Residual solvent was removed by storing the lipid film under vacuum overnight. An appropriate volume of PBS, pH 7.4, was added to the thin lipid film to give the required final concentration of DMPC. The lipid-peptide complexes were prepared by adding the required volume of peptide solutions to give a lipid to peptide molar ratio of 20:1. Due to the poor solubility of these peptides, a peptide concentration of 11 μM was used. The mean residue ellipticity, $[\theta]_{MRE}$ (deg.cm^2.dmol^{-1}) at 222 nm, was calculated using the following equation:

$$[\theta]_{MRE} = MRW[\theta]/10cl$$

where MRW is mean residue weight of the peptide, θ is the observed ellipticity in degrees, c is the concentration of the peptide in g/ml, and l is the path length of the cell in centimeters. The percent helicity of the peptide was estimated from the following equation as described by Morrisett et al. (32):

$$\%\ \alpha\ \text{helicity} = ([\theta]_{222} + 3{,}000)/(36{,}000 + 3{,}000)$$

where $[\theta]_{222}$ is the mean residue ellipticity at 222 nm.

Differential scanning calorimetry

Differential scanning calorimetry (DSC) studies were carried out using a Microcal MC-2 scanning calorimeter (MicroCal, Inc., Amherst, MA) at a scan rate of 20°C h^{-1} for DMPC, and 37°C h^{-1} for Di (16:1) palmitoleoyl phosphatidylethanolamine (DiPoPE), using the procedure described by Mishra et al. (28). A known

amount of phospholipid was dissolved in chloroform. For one set of samples, peptide was dissolved in methanol and added to a solution of DiPoPE in chloroform–methanol (2:1, v/v). For both, pure lipid samples and the organic solutions of lipid and peptide, solvent was removed under a slow stream of nitrogen. Residual solvent was removed under vacuum. Buffer [PBS, pH 7.4, for DMPC or 20 mM PIPES, 1 mM EDTA, 150 mM NaCl, and 0.002% NaN_3, pH 7.4, for DiPoPE] alone or a known concentration of peptide solution in buffer to give a specific lipid/peptide molar ratio was added to the dried film and hydrated by vortexing at room temperature for 30 min. For DMPC, four consecutive scans with a 60 min equilibration time between scans were taken. DSC thermograms were analyzed using the software provided by MicroCal Inc. and Origin, version 5.0.

Surface pressure measurements

Monolayer exclusion pressure measurements give the affinity of the peptides for a lipid-water interface; the procedure of Phillips and Krebs (33, 34) was followed. An insoluble monolayer of egg phosphatidylcholine (EPC) was spread at the air-water interface in a Teflon dish at room temperature to give an initial surface pressure (π_i) in the range of 5–45 dyn/cm. A solution of peptides in PBS containing 1.5 M guanidine hydrochloride (Gdn.HCl) was carefully injected in to the subphase to give a final concentration of 50 μg/dl. The Gdn.HCl was diluted in the subphase to a final concentration of ≤1 mM to allow the peptides to renature. The subphase was stirred continuously and the increase in EPC monolayer surface pressure ($\Delta\pi$) was recorded until a steady state value was obtained. The value of the initial surface pressure (π_i) at which the peptides no longer penetrate the EPC monolayer [i.e., the exclusion pressure (π_e)], was calculated by extrapolating the π_i versus $\Delta\pi$ linear regression fit to $\Delta\pi = 0$ dyn/cm.

Right angle light scattering measurements

Association of these peptides with egg phosphatidylcholine was determined by following the dissolution of EPC multilamellar vesicles (MLV) by right angle light scattering using a SLM 8000C photon counting spectrofluorometer as described in (28). EPC MLVs were prepared by evaporating a solution of EPC (Avanti Polar, AL) under nitrogen and hydrating the lipid film with phosphate-buffered saline (pH 7.4). The sample containing 105 μM EPC and an equimolar amount of peptide was maintained at 25°C and continuously stirred. Turbidity clarification was monitored for 30 min. Complete dissolution of EPC vesicles was achieved by addition of Triton X-100 to a final concentration of 1 mM.

LCAT purification

LCAT was isolated from fresh normolipidemic plasma by the method of Albers et al. (35) with some modifications. The density of the plasma was adjusted to 1.21 g/ml and it was centrifuged at 175,000 g for 24 h. The LCAT containing fraction was subjected to Affi-Gel Blue chromatography followed by DE-52 chromatography. LCAT was eluted from the DE-52 column using a 75 to 200 mM NaCl gradient in Tris buffer (10 mM, pH 7.6). SDS-PAGE showed greater than 90% purity of the enzyme with no human apoA-I contamination.

Assay of LCAT activity

The substrate was prepared by sonicating EPC/cholesterol (90:20 mol/mol) containing trace amounts of 7α-[^{3}H]cholesterol in a Branson 250 sonifier for 12 min to obtain small unilamellar vesicles. The substrate (50 μl) was incubated with 5 μg of peptide or human apoA-I and 50 μl of bovine serum albumin (BSA) (40 μg/ml) for 1 h at 37°C. The total volume was brought up to 150 μl. After incubating for 1 h, 100 μl of LCAT was added and incubated for 1 h at 37°C and the reaction was quenched by spotting 10 μl on a silica strip. Cholesterol and cholesteryl ester were separated by thin layer chromatography of the silica strip in hexane–chloroform (2:1, v/v) mixture. Cholesterol and cholesteryl oleate standards were visualized by immersing the thin-layer chromatography plate in a 3% cupric acetate, 8% phosphoric acid buffer, and heating it. The positions of the standards were used to cut the strip into two and the two parts were counted in scintillation fluid in a Packard Tri Carb 4530. All reactions were done in triplicate. The activation of LCAT by the peptides is expressed as a percentage of the total activation by apoA-I.

Electrophoresis

Nondenaturing and SDS-PAGE was carried out using the method of Laemmli (36). Premade Novex gels were used and the gel was stained with Coomassie blue to identify the protein bands.

LDL-induced monocyte chemotactic activity

Cocultures of human artery wall cells, monocyte isolation, isolation of lipoproteins by ultracentrifugation from the plasma of normal human donors or from mouse plasma by FPLC, and determination of lipid hydroperoxides and monocyte chemotactic activity were performed as previously described (37, 38). Briefly, LDL and HDL were isolated from human plasma by the method of Havel et al. (39). Human aortic endothelial cells (HAEC) and human aortic smooth muscle cells (HASMC) were isolated as previously described (37). Microtitre plates were treated with 0.1% gelatin at 37°C overnight. HASMC were added at a confluent density of 1×10^5 cells/cm^2. Cells were cultured for two days, at which time they had covered the entire surface of the well and had produced a substantial amount of extracellular matrix. HAEC were subsequently added at 2×10^5 cells/cm^2 and were allowed to grow, forming a complete monolayer of confluent HAEC in two days. In all experiments, HAEC and autologous HASMC (from the same donor) were used at passage levels of four to six. Monocytes were isolated blood from normal donors as described by us earlier (40). The cocultures were treated with native LDL (250 μg protein/ml) or presence of HDL (350 μg protein/ml) or peptides for 8 h. The cocultures were then washed and incubated with medium 199 for an additional 8 h. The resulting coculture supernatants were assayed for monocyte chemotactic activity as described previously (41).

RESULTS

Analysis of the peptides

Table 1 shows the sequences of the various 18A analogs that were synthesized. The peptide Ac-18A-NH_2, which has two Phe residues at positions 6 and 18 (close to the interfacial Lys residues), is referred to as 2F. Two 3F peptides were synthesized, 3F^3 or 3F^{14}, where Leu in positions 3 and 14 (both present at the center of the nonpolar face) is replaced by Phe, respectively. Peptide 4F has two Phe residues at the center of the nonpolar face, which is a result of substitution of two central Leu residues. The substitutions in the peptides (3F to 7F) are shown in Table 1. With an increase in the number of Phe residues, the theoretical hydrophobicity per residue on the nonpolar face increases from 2.05 for the peptide 2F, to 3.15 for 7F.

TABLE 1. Modifications of Ac-18A-NH_2 to increase hydrophobicity

Peptide	Sequence[a]	Hydrophobicity[b]	Theoretical Lipid Affinity [c]
			Λ
2F	Ac-18A-NH_2	2.05	13.03
$3F^3$	Ac-[$F^3$18A]-NH_2	2.20	13.84
$3F^{14}$	Ac-[F^{14}18A]-NH_2	2.20	13.79
4F	Ac-[$F^{3,14}$18A]-NH_2	2.35	14.59
5F	Ac-[$F^{11,14,17}$18A]-NH_2	2.81	19.07
6F	Ac-[$F^{10,11,14,17}$18A]-NH_2	2.96	19.87
7F	Ac-[$F^{3,10,11,14,17}$18A]-NH_2	3.15	20.78

[a] Baseline sequence 18A DWLKAFYDKVAEKLKEAF.
[b] Hydrophobicity is expressed as the hydrophobicity per residue on the nonpolar face.
[c] Theoretical lipid affinity has been calculated as shown in (44).

The peptides were purified on a preparative Vydac C_4 column by RP-HPLC using water (with 0.1% trifluoroacetic acid) and acetonitrile (0.1% trifluoroacetic acid). The purity and the retention times of the peptides were determined on an analytical Vydac C_{18} column using a gradient of 25% to 58% acetonitrile in water containing 0.1% TFA. The purity of these peptides was also confirmed by mass spectrometry. The mass was in agreement with the calculated molecular weight. The retention times of the peptides are listed in **Table 2**. Although both the 3F peptides and 4F have additional Phe residues compared with 2F, the retention times of these peptides on the C_{18} column are not very different (~22 min). A sudden increase in the retention time is apparent with 5F, 6F, and 7F (~26 min). With the increase in number of Phe residues, the solubility of these peptides in PBS decreases. As can be seen from Table 2, the solubility of 2F, $3F^3$, $3F^{14}$, and 4F (1.25 to 1.4 mg/ml) are significantly higher than those of 5F, 6F, and 7F (0.03 to 0.1 mg/ml).

The self-association of these amphipathic peptides was examined by nondenaturing polyacrylamide gel electrophoresis (PAGE) **Fig. 1** shows the mobility of 2F on both denaturing SDS (Fig. 1A) and on nondenaturing (Fig. 1B) gels. The molecular mass of 2F is 2242 and it can be seen as a single band on the SDS gel (Fig. 1A) moving slightly lower than the lowest molecular mass standard (3.5–2.5 kDa). However, under nondenaturing conditions it forms aggregates in a concentration dependent manner as seen in Fig. 1B. At lower concentrations (100 μg/ml) it forms aggregates of two sizes while at a higher concentration (250 μg/ml) only the bigger aggregates are observed (Fig. 1B). All the other peptides studied also exhibited aggregation under nondenaturing conditions, suggesting that the peptides possess a strong tendency to self-associate.

TABLE 2. Physical properties of the F-peptides

Peptide	Molecular Weight[a]	Retention Time[b]	Solubility[c]	Monolayer Exclusion Pressure (π_e)[d]
		min	*mg/ml*	*dyn/cm*
ApoA-I	28,000	28.0	>2.0	34
18A	2,200	19.8	>2.0	30
37pA	4,580	26.0	>2.0	41
2F	2,242	22.5	>2.0	38
$3F^3$	2,276	21.0	1.25	38
$3F^{14}$	2,276	21.2	1.45	39
4F	2,310	22.0	1.30	40
5F	2,429	26.5	0.10	45
6F	2,462	27.0	0.03	46
7F	2,510	26.0	0.10	45

[a] The mass as determined by mass spectroscopy was very close to the theoretically calculated molecular weight.
[b] The retention time is the time taken for the peptide to elute from a Vydac C_{18} column using the gradient 25% to 58% of acetonitrile in water containing 0.1% TFA in 33 min.
[c] Solubility was determined in PBS.
[d] Reproducibility of these measurements is ±1 dyn/cm.

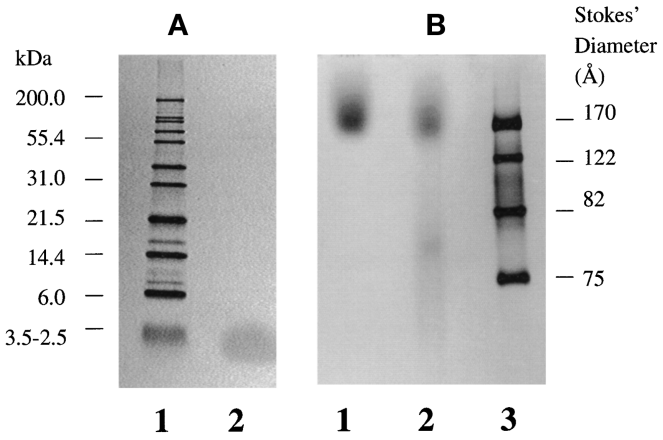

Fig. 1. Electrophoresis of 2F indicating its self-association. A: SDS PAGE (18%) of 2F. Lane 1 shows the molecular mass standard and lane 2 shows the band corresponding to 2F (molecular mass is 2242) moving slightly lower than the lowest molecular mass standard (3.5–2.5 kDa). B: Nondenaturing PAGE (4–12%) showing the mobilities of 100 μg/ml (lane 2) and 250 μg/ml (lane 1) of 2F indicating self-association in solution. Lane 3 shows the mobility of the high molecular mass standard.

Circular dichroism

The secondary structure of the peptides was determined by circular dichroism spectroscopy. **Table 3** shows the percent helicity of the peptides in PBS and in the presence of DMPC. In PBS, homologues 2F, 4F, 5F, 6F, and 7F have a higher percentage helicity than $3F^3$ and $3F^{14}$ (Table 3). Because 5F, 6F, and 7F were sparingly soluble in PBS, the CD studies were carried out using 11μM of the peptides (a concentration at which they were all soluble). Peptide 2F showed 55% helicity, comparable to 5F in solution. Both 6F and 7F were slightly more helical (67% and 58%, respectively) whereas 4F was slightly less (45%). Both the 3F peptides were much less (~20%) helical. However, binding to DMPC considerably increased the helicity of all the peptides except for 6F (Table 3). In a lipid environment, 2F, 5F, and 7F showed a high helical content (68% to 76%). Although, the peptides $3F^3$ and $3F^{14}$ had a very small helical content in PBS, there was a significant increase in helicity in a lipid environment, from about 22% to 42% for $3F^3$, and from 19% to 55% for $3F^{14}$. The helicity of the peptides 6F and 4F did not change appreciably in the presence of lipid. However, these peptides were still less helical than peptides 2F and 5F. The CD

TABLE 3. Helicities of the F-peptides in aqueous and lipid environments

Peptides	Percent Helicity	
	PBS[a]	DMPC[a]
2F	55	72
$3F^3$	22	42
$3F^{14}$	19	55
4F	45	44
5F	55	76
6F	67	50
7F	58	68

[a] 11 μM solutions of peptide was used. Peptide:DMPC ratio used was 1:20 (mol/mol). Three measurements were made and an error of ±10% was obtained.

results suggest that there is no systematic change in the helicities of the peptides with increasing substitution by Phe; peptides 2F and 5F exhibited maximum helicity in solution and in the presence of phospholipid.

DSC studies with DMPC and DiPoPE

The effect of these 18A analogs on the chain melting transition of multilamellar vesicles of DMPC was studied by DSC using peptide-lipid mixtures at 100:1 lipid/peptide molar ratio. **Table 4** shows the transition temperatures and enthalpies of the chain melting transition of DMPC in the presence and absence of peptides. The pure lipid undergoes a pretransition at 13°C and a main chain melting transition at 23°C. The addition of the peptides to DMPC resulted in a broadening of the gel to liquid-crystalline transition and a lowering of the transition enthalpy (Table 4). The pretransition was not seen in the presence of any of the peptides. Among the peptides studied, 2F, $3F^3$, 5F, and 6F reduced the transition enthalpy to the maximum extent (Table 4). None of the peptides changed the transition temperature by more than 0.2°C.

The shift in the bilayer to hexagonal phase transition temperature (T_H) has been used to evaluate the effects of peptides on the intrinsic curvature properties of phospholipids (42). It was previously shown that 2F raises T_H of DiPoPE (43). In the current study, we prepared the peptide-lipid mixtures in two ways. One was by adding the peptide in organic solvent to the lipid in organic solvent

TABLE 4. Effect of the F-peptides on the chain melting transition parameters of DMPC

Peptide	T_{CM}	ΔH_{CM}	$\Delta_{T1/2}$
	°C	*kcals/mol*	*°C*
DMPC	23.1	6.4	0.2
2F	23.2	4.5	0.5
$3F^3$	23.2	4.9	0.4
$3F^{14}$	23.2	5.5	0.3
4F	23.2	5.3	0.4
5F	23.2	4.9	0.5
6F	23.1	4.0	0.5
7F	23.2	4.5	0.5

The DMPC/peptide ratio used was 100:1 (mol/mol). The concentration of the DMPC used was 1.5 mM. T_{CM} is the temperature at which the chain melting transition takes place, ΔH_{CM} is the enthalpy of the transition, and $\Delta_{T1/2}$ is the width at half maximum of the transition.

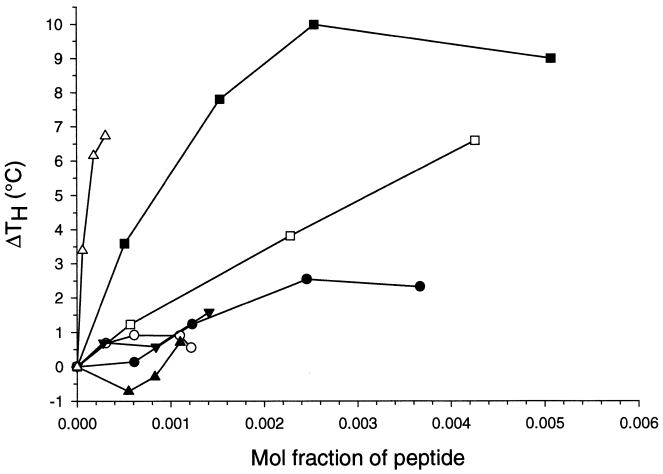

Fig. 2. The homologous series of peptides stabilize the hex-phase transition of DiPoPE bilayers. Shift in T_H of DiPoPE as a function of the mole fraction of added peptide. Measured by DSC at a heating scan rate of 37°C/h. 2F (solid circle); $3F^3$ (open circle); 4F (solid square); 5F (open square); 6F (inverted solid triangle); 7F (solid triangle); apoA-I (open triangle).

followed by depositing the material as a film and subsequently hydrating with buffer. In the other method, the peptide and lipid were mixed after each was hydrated separately. If the mixture comes to equilibrium prior to the DSC analysis, it should not matter how the peptide and lipid are originally mixed. However, membrane systems can equilibrate slowly, in which case there may be more peptide in the lipid when it was incorporated at high concentrations into the lipid film. In general, the results from both methods of sample preparation are similar (not shown) but the shift in T_H tends to be larger for samples in which peptide was incorporated into a film composed of lipid and peptide. The variation of the T_H with mol fraction of peptide is shown for the various peptides and apoA-I (**Fig. 2**). A linear increase in T_H is observed for 2F and 5F, whereas 4F behaves more like apoA-I in that a more rapid increase is observed at lower peptide concentrations. On the other hand, the two 3F analogs as well as 6F and 7F do not significantly affect T_H.

Interaction of peptides with phospholipid monolayers

The monolayer exclusion pressure, π_e, is the surface pressure at which peptides are no longer able to penetrate a monolayer of EPC. The value of π_e reflects the theoretical lipid affinity of the peptide. The exclusion pressure of the F peptides increased with the increase in number of Phe residues (Table 2). All the peptides studied here had higher exclusion pressures than apoA-I and the parent peptide 18A. The value of π_e increased gradually from 2F to 4F (38 to 40 dyn/cm). This is in the range seen for 37pA, a tandem repeat of 18A punctuated by a proline. The exclusion pressure value increases significantly for 5F, 6F, and 7F (40 to 45 dyn/cm). It is apparent that the 5F, 6F, and 7F homologues possess a similar ability to interact with EPC monolayers, as determined by the exclusion pressure. It is interesting that the HPLC retention times and monolayer exclusion pressures for the F-peptides listed in

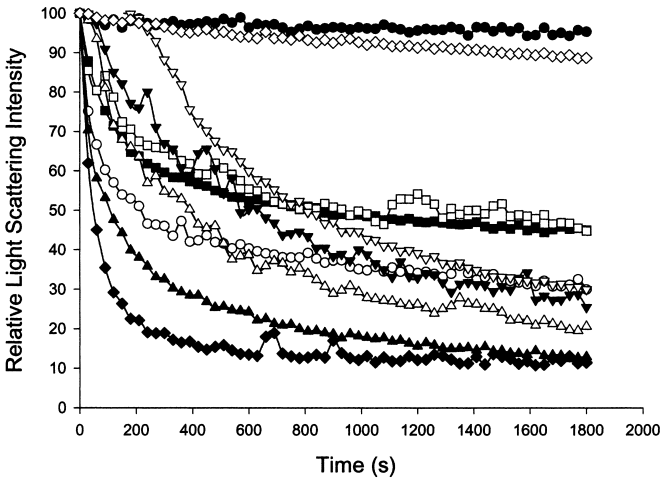

Fig. 3. Relative right angle light scattering monitoring of the dissolution of EPC MLVs by homologous series of peptides as a function of time. A representative EPC MLV clarification curve is shown for each of the homologous peptides. An equimolar concentration of peptide and EPC was used (105 μM). Both excitation and emission wavelengths were 400 nm. Triton X-100 achieved complete dissolution at a final concentration of 1 mM. EPC (solid circle); 2F (open circle); $3F^3$ (solid square); $3F^{14}$ (open square); 4F (solid triangle); 5F (open triangle); 6F (inverted solid triangle); 7F (inverted open triangle); human apoA-I (open diamond); Triton X-100 (solid diamond.

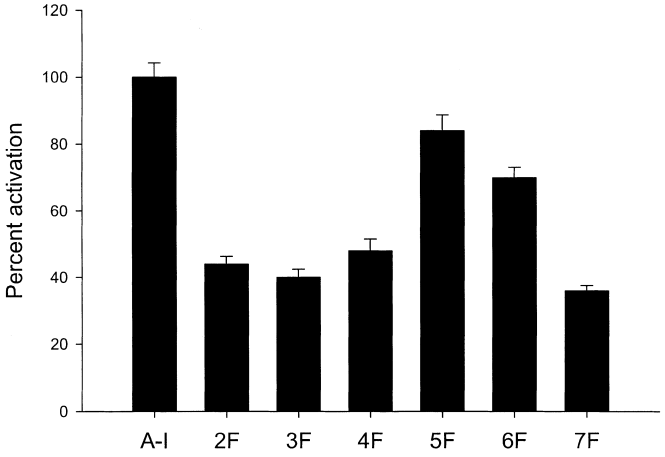

Fig. 4. LCAT activating ability of homologous peptides. Histograms representing activation of LCAT by the F-peptides. LCAT activity was measured using small unilamellar vesicles of EPC-cholesterol and the activity is represented as a percentage compared with that of apoA-I activity, where apoA-I activity is taken to be 100%. Each value is an average of three values. The peptide concentration used was 20 μg/ml. Error bars represent ± SEM values.

Table 2 show parallel trends, with an abrupt increase between 4F and 5F.

Right angle light scattering

As can be seen in **Fig. 3**, all the peptides were able to clarify EPC MLVs, unlike apoA-I, which does not clarify EPC MLVs. The two homologous 3F peptides were the least effective in clarifying the EPC MLVs. The homologous peptides 2F, 5F, 6F, and 7F all clarified the EPC MLVs to similar extents. Peptide 4F was the most effective in clarifying EPC MLVs with activity similar to that of Triton X-100. The time for 50% clearance of the turbidity of EPC MLVs was also the shortest for the homologue 4F. Peptide 7F took the longest time to achieve 50% clearance; this was because of an initial lag period of ~300 s (Fig. 3). This is probably due to the requirement for self-associated 7F molecules to dissociate before they can interact with EPC MLVs and solubilize them. The slower rates of clearance exhibited by the homologues 2F, 5F, and 6F may also be due to a higher self-association of these peptides.

Activation of the plasma enzyme LCAT

The ability of these peptides to activate the plasma enzyme LCAT was determined by measuring the initial velocity of the LCAT reaction with EPC-cholesterol vesicles as substrate (**Fig. 4**). LCAT activation is expressed relative to that by apoA-I, which was considered to be 100%. Activation of LCAT by 20 μg/ml of peptides and apoA-I is shown in Fig. 4. At this concentration, apoA-I activates LCAT better than any of the peptides. Among the peptides studied here, however, 5F is the best activator (80% of apoA-I). As far as LCAT activation is concerned, both $3F^3$ and $3F^{14}$ have similar activating abilities. Therefore, they have been represented as one bar (Fig. 4).

LDL-induced monocyte chemotactic activity

When LDL is incubated with the human artery wall coculture system, it is trapped in the subendothelial space and gets oxidized to produce biologically active lipids. These lipids induce monocyte chemotaxis. Thus, coculture monocyte chemotaxis is a well-established assay for the formation of biologically active lipids. It has been shown that inhibition of chemotaxis is directly correlated with the removal of "seeding molecules" that are responsible for the secretion of monocyte chemotactic protein-1 (MCP-1) (21, 22) and differentiation factor macrophage colony-stimulating factor (M-CSF). **Fig. 5** shows that LDL after incubation with peptides exhibited varied effects with homologues 4F, 5F, and 6F, reducing the chemotactic properties of LDL the most. Peptides 3F were not at all effective compared with 2F and 7F, which were less effective than the peptides 4F, 5F, and 6F.

DISCUSSION

Effect of increasing hydrophobicity of a class A amphipathic helical peptide analog on its physical-chemical and lipid binding properties

The peptides studied in this paper are homologues of the parent peptide, 18A . The calculated hydrophobicity per residue [according to modified GES scale (44)] on the nonpolar face increased as the number of Phe residues increased. This increase in hydrophobicity (Table 1) is reflected in the theoretical lipid affinity, Λ (44). However, the Λ value increases gradually from 2F to 4F (from 13.03 to 14.59) with a sudden increase in the value from 14.59 (for 4F) to 19.07 for 5F. A gradual increase in Λ was again

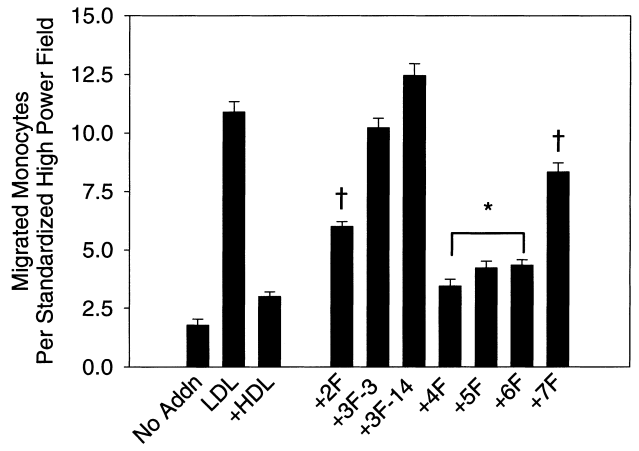

Fig. 5. LDL-induced monocyte chemotaxis inhibited by the homologous series of peptides. LDL alone or LDL incubated with either human HDL or the homologous series of peptides was added to the human artery wall cell cocultures for 8 h in the presence of 10% lipoprotein-deficient serum. The supernatants were removed and the cocultures were washed with culture medium without serum or LPDS. The conditioned medium was then collected and analyzed for monocyte chemotactic activity. The data represent mean ± SEM values (n = 9 in each case). By pair-wise comparisons with LDL, all peptides except the 3F peptides were significantly more effective (at least $P < 0.001$, signified by † and *). Comparisons between all peptides were analyzed by one-way ANOVA. The asterisk indicates that peptides 4F, 5F, and 6F were significantly more effective than the homologues 2F and 7F ($P < 0.05$ by Duckett comparison). The bracket indicates no significant difference in the ability to inhibit LDL-induced chemotaxis among these three peptides.

observed after 5F in the values for 6F and 7F (Table 1). This is due to the substitution of Leu at positions 3 and 14 in Ac-18A-NH_2 with Phe, which results in a slight increase in the hydrophobicity of the nonpolar face and thus a slight increase in Λ values for the two 3F analogs and 4F. In homologues 5F, 6F, and 7F however, besides the Leu to Phe substitutions, Ala in positions 11 and 17 are also substituted by Phe, resulting in a significant increase in the Λ values (Table 1). Because Ala is less hydrophobic than Leu and Leu is less hydrophobic than Phe, the substitution of Ala to Phe causes a greater change in hydrophobicity and theoretical lipid affinity of the resulting peptide than a Leu to Phe substitution.

The retention time on a C_{18} reversed phase HPLC column, solubility of these peptides, and their ability to penetrate an EPC monolayer all exhibit a trend similar to that seen in the theoretical lipid affinity values (Table 2). The retention times of peptides 2F, $3F^3$, $3F^{14}$, and 4F are about the same (21–22 min) and significantly less than those of 5F, 6F, and 7F, which comprise a second group (26–27 min). The peptides 2F to 4F have considerably higher aqueous solubility than homologues 5F to 7F, which are sparingly soluble (Table 2). A gradual increase in exclusion pressure was observed from 2F to 4F after which there is an abrupt increase from 40 dyn/cm to 45 dyn/cm. The exclusion pressures for the peptides 5F, 6F, and 7F are not very different from each other and are significantly higher than that of apoA-I (Table 2). The parent peptide 18A (30 dyn/cm) and even the dimer of 18A, 37pA (40 dyn/cm) were also significantly less effective in penetrating into an egg PC monolayer spread at the air-water interface. Based on the above physical properties, the F peptides can be separated into two groups: group 1 with 2F, $3F^3$, $3F^{14}$, 4F and group 2 with peptides 5F, 6F, and 7F.

The CD data (Table 3) indicate that the percent helicity value of all the peptides increases in the presence of DMPC, suggesting that all of the peptides associate with lipids. The binding of these peptides to DMPC appears to be similar as suggested by DSC (Table 4). However, the effect of these peptides on the stabilization of the bilayer structure of DiPoPE is different. 4F and 5F seem to interact better with DiPoPE because they appear to be better stabilizers than the other peptides.

Whereas apoA-I is not able to clarify EPC MLVs, all of the peptide analogs are able to do so, but to different extents. Among the group 1 peptides that are easily soluble in aqueous buffer and exhibit a monolayer exclusion pressure value in the range 38–40 dyn/cm (2F, 3F analogs, and 4F), 4F appears to be the most efficient and at the peptide-lipid ratio under investigation, exhibits similar kinetics to that of Triton X-100 (Fig. 3). Whereas the monolayer exclusion pressures of the peptides 2F and 3F are similar, the 3F homologues are the slowest in clarifying EPC MLVs. The reason for reduced EPC clarifying ability of the 3F homologues is not clear at this time. The group 2 peptides (5F, 6F, and 7F) that are not easily soluble in aqueous buffer and possess surface pressure values 45 dyn/cm solubilize EPC MLVs relatively slowly. These results are consistent with peptide aggregates having to disassociate and then interact with EPC. The superior reactivity of 4F can be explained by the fact that its hydrophobicity is optimal so that hydrophobic peptide-peptide interactions favoring self-association do not prevent peptide-lipid interactions.

Effect of increased hydrophobicity on LCAT activation

Activation of LCAT is a complex process and is not only dependent on lipid affinity but also on the interaction of the amphipathic helical protein with the enzyme LCAT (45). In agreement with this, the ability to activate LCAT was found to be different for the homologous peptides. The peptide 5F showed the maximum LCAT-activating ability, in agreement with the physical properties studied in Table 2 wherein an abrupt increase was seen from 4F to 5F, including exclusion pressure values at the egg PC-water interface. The fact that the peptides 6F and 7F are not as effective as 5F could be explained by the increased peptide-peptide interaction (as reflected in the low aqueous solubility of these peptides), which does not allow for peptide-lipid or peptide-LCAT interaction. These results are in agreement with our earlier observations with the 18A dimer peptides in which the enhanced self-association of the dimer 18A-18A (36A) peptide reduced its ability to interact with lipids compared with 18A-Pro-18A peptide (29). Although LCAT activation by the peptides has been compared with that of apoA-I, it should be noted that apoA-I and the peptides interact differently with the substrate because they all have different reactivities to

EPC (Fig. 3). Similar observations were made by Chung et al. who showed that a synthetic peptide 18A-Pro-18A and apoA-I interact differently with EPC (46).

Effect of increased hydrophobicity of the nonpolar face on LDL-induced monocyte chemotaxis

Because removal of "seeding molecules" depends on the amphipathicity of the peptide as reported by us (21, 22), we examined the ability of these peptides to inhibit LDL-induced monocyte chemotaxis. In this assay, peptides 4F, 5F, and 6F at 100 μg/ml level showed significant and similar inhibition of LDL-induced chemotaxis based on one way analysis of variance. Although the homologue 2F showed some inhibitory activity, for reasons that are not clear, peptide analogs 3F showed no inhibition compared with LDL alone. These results were in agreement with the fact that the peptide 3F was not able to remove the lipid hydroperoxides (results not shown) and the reduced ability to clarify EPC MLVs. Peptide 7F was significantly less effective than peptides 4F, 5F, and 6F ($P < 0.001$). The reduced ability of 7F can again be explained by increased self-association of the peptide that decreased its ability to interact with the lipid as seen in EPC MLV clarification studies. These results again demonstrate that the delicate balance existing between the contributions of the hydrophobicity of the peptide to self-association can critically affect apoA-I-mimicking properties.

In vivo administration of peptide 5F, which possesses increased LCAT-activating ability and increased ability to remove "seeding molecules," protected mice from diet-induced atherosclerosis (20). In contrast, administration of 2F, which is similar in LCAT-activating ability to 4F but less effective than 4F and 5F in removing "seeding molecules" from LDL, did not significantly inhibit diet-induced lesion formation in C57 BL6 mice (mean lesion area for control mice administered with PBS $14.7 \pm 1.8\ \mu m^2 \times 10^{-3}$ compared with 2F-administered mice $13.2 \pm 1.7\ \mu m^2 \times 10^{-3}$, $n = 15$) (47). It follows that in this mouse model, inhibition of LDL-induced monocyte chemotaxis is more antiatherogenic than LCAT activation. Because the peptides 2F and 4F are similar in activating LCAT, and 4F and 5F are similar in removing "seeding molecules" from LDL, the peptide 4F may serve as a reagent to distinguish between the importance of LCAT activation and the inhibition of LDL-induced monocyte chemotaxis in different atherosclerosis-sensitive mouse models. If the inhibition of LDL-induced chemotaxis is more important than the LCAT-activating ability, then 4F should be the better peptide to use as an inhibitor of atherosclerosis because this peptide is more soluble than the peptides 5F, 6F, and 7F.

We thank the Comprehensive Cancer core facility, University of Alabama at Birmingham Medical Center, for mass spectral analysis of synthetic amphipathic helical peptides. This work was supported in part by NIH grants HL34343, HL22633, HL30568, and Medical Research Council of Canada grant MT-7654.

Manuscript received 22 December 2000 and in revised form 9 March 2001.

REFERENCES

1. Sprecher, D. L., H. S, Feigelson, and P. M. Laskarzewsli. 1993. The low HDL cholesterol/high triglyceride trait. *Arterioscler. Thromb.* **13:** 495–504.
2. Philips, N. R., D. Waters, and R. J. Havel. 1993. Plasma lipoproteins and progression of cardiovascular disease evaluated by angiography and clinical events. *Circulation.* **88:** 2762–2770.
3. Segrest, J. P., H. De Loof, J. G. Dohlman, C. G. Brouillette, and G. M. Anantharamaiah. 1990. Amphipathic helix motif: Classes and Properties. *Proteins.* **8:** 103–117.
4. Anantharamaiah, G. M., M. K. Jones, and J. P. Segrest. 1993. An atlas of the amphipathic helical domains of human exchangeable plasma apolipoproteins. *In* The Amphipathic Helix. R. M. Epand, editor. CRC Press, Boca Raton, FL. 109–142.
5. Segrest, J. P., M. K. Jones, H. De Loof, C. G. Brouillette, Y. V. Venkatachalapathi, and G. M. Anatharamaiah. 1992. The amphipathic helix in exchangeable apolipoproteins: a review of secondary structure and function. *J. Lipid Res.* **33:** 141–166.
6. Segrest, J. P., D. W. Garber, C. G. Brouillette, S. C. Harvey, and G. M. Anatharamaiah. 1994. The amphipathic helix: the multifunctional and structural motif in plasma apolipoproteins *Adv. Prot. Chem.* **45:** 303–369.
7. Brouillette, C. G., and G. M. Anantharamaiah. 1995. Structural models of human apolipoprotein A-I. *Biochim. Biophys. Acta.* **1256:** 103–129.
8. Mishra, V. K., M. N. Palgunachari, G. Datta, M. C. Phillips, S. Lund-Katz, S. O. Adeyeye, J. P. Segrest, and G. M. Anantharamaiah. 1998. Studies of synthetic peptides of human apolipoprotein A-I containing tandem amphipathic α helixes. *Biochemistry.* **37:** 10313–10324.
9. Borhani, D. W., D. P. Rogers, J. A. Engler, and C. G. Brouillette. 1999. Crystal structure of truncated human apolipoprotein A-I suggests a lipid bound conformation. *Proc. Natl. Acad. Sci. USA.* **94:** 12291–12296.
10. Segrest, J. P., L. Li, G. M. Anantharamaiah, S. C. Harvey, K. N. Liadaki, and V. Zainis. 2000. Structure and function of apolipoprotein A-I and high density lipoprotein. *Current Opin. Lipidol.* **11:** 105–115.
11. Brouillette, C. G., G. M. Anantharamaiah, J. A. Engler, and D. W. Borhani. 2001. Structural models of human apolipoprotein A-I: a critical analysis and review. *Biochim. Biophys. Acta.* **1531:** 4–46.
12. Fielding, C. J., and P. E. Fielding. 1995. Molecular physiology of reverse cholesterol transport. *J. Lipid Res.* **36:** 211–228.
13. Glomset, J. A. 1968. The plasma lecithins:cholesterol acyltransferase reaction. *J. Lipid Res.* **9:** 155–167.
14. Johnson, W. J., F. H. Mahlberg, G. H. Rothblat, and M. C. Phillips. 1991. Cholesterol transport between cells and high density lipoproteins. *Biochim. Biophys. Acta.* **1085:** 273–298.
15. Oram, J. F., and S. Yokoyama. 1996. Apolipoprotein-mediated removal of cellular cholesterol and phospholipids. *J. Lipid Res.* **37:** 2473–2491.
16. Fielding, C. J., V. G. Shore, and P. E. Fielding. 1972. A protein cofactor of lecithin:cholesterol acyltransferase. *Biochem. Biophys. Res. Comm.* **46:** 1493–1498.
17. Jonas, A. 1991. Lecithin:cholesterol acyltransferase in the metabolism of high density lipoproteins. *Biochim. Biophys. Acta.* **1084:** 205–220.
18. Kreiger, M. 1999. Charting the fate of the "Good cholesterol": identification and characterization of the high-density lipoprotein receptor SR-BI. *Ann. Rev. Biochem.* **68:** 523–558.
19. Shah, P. K., J. Nilsson, S. Kaul, M. C. Fishbein, H. Ageland, A. Hamsten, J. Hohansson, F. Karpe, and B. Cereck, 1998. Effects of recombinant apolipoprotein A-Imilano on aortic atherosclerosis in apolipoprotein E-deficient mice. *Circulation.* **97:** 780–785.
20. Garber, D. W., G. Datta, M. Chaddha, M. N. Palgunachari, S. Y. Hama, M. Navab, A. M. Fogelman, J. P. Segrest, and G. M. Anantharamaiah. 2001. A new synthetic class A amphipathic helical peptide analog protects mice from diet-induced atherosclerosis. *J. Lipid Res.* **42:** 545–552.
21. Navab, M., S. Y. Hama, C. J. Cooke, G. M. Anantharamaiah, M. Chaddha, L. Jin, G. Subbanagounder, K. F. Faull, S. Reddy, N. E. Miller, A. M. Fogelman. 2000. Normal high density lipoprotein inhibits three steps in the formation of mildly oxidized low density lipoprotein: step 1. *J. Lipid Res.* **41:** 1481–1494.
22. Navab, M., S. Y. Hama, G. M. Anantharamaiah, K. Hassan, G. P. Hough, A. D. Watson, S. T. Reddy, A. Sevanian, G. C. Fonarow, and

A. M. Fogelman. 2000. Normal high density lipoprotein inhibits three steps in the formation of mildly oxidized low density lipoprotein: steps 2 and 3. *J. Lipid Res.* **41:** 1495–1508.
23. Anantharamaiah, G. M., Y. V. Venkatachalapathi, C. G. Brouillette, and J. P. Segrest. 1990. Use of synthetic peptide analogues to localize lecithin:cholesterol acyltransferase activating domain in apolipoprotein A-I. *Arteriosclerosis.* **10:** 95–105.
24. Epand, R. M., A. Gawish, M. Iqbal, K. B. Gupta, C. H. Chen, J. P. Segrest, and G. M. Anantharamaiah. 1987. Studies of synthetic peptide analogs of the amphipathic helix. *J. Biol. Chem.* **262:** 9389–9396.
25. Davidson, S. W., S. Lund-Katz, W. J. Johnson, G. M. Anantharamaiah, M. N. Palgunachari, J. P. Segrest, G. H. Rothbalt, and M. C. Phillips. 1994. The influence of apolipoprotein structure on the efflux of cellular free cholesterol to high density lipoprotein. *J. Biol. Chem.* **269:** 22975–22982.
26. Yancey, P. G., J. K. Bielicki, S. Lund-Katz, M. N. Palgunachari, G. M. Anantharamaiah, J. P. Segrest, M. C. Phillips, and G. H. Rothblat. 1995. Efflux of cellular cholesterol and phospholipid to lipid-free apolipoproteins and class A amphipathic peptides. *Biochemistry.* **34:** 7955–7965.
27. Venkatachalapathi, Y. V., M. C. Phillips, R. M. Epand, R. F. Epand, E. M. Tytler, J. P. Segrest, and G. M.Anantharamaiah. 1993. Effect of end group blockage on the properties of a class A amphipathic helical peptide. *Proteins: Structure, Function and Genetics.* **15:** 349–359.
28. Mishra, V. K., M. N. Palgunachari, J. P. Segrest, and G. M. Anantharamaiah. 1994. Interactions of synthetic peptide analogs of the class A amphipathic helix with lipids. *J. Biol. Chem.* **269:** 7185–7191.
29. Mishra, V. K., M. N. Palgunachari, S. Lund-Katz, M. C. Phillips, J. P. Segrest, and G. M. Anantharamaiah. 1995. Effect of the arrangement of tandem repeating units of class A amphipathic helixes on lipid interaction. *J. Biol. Chem.* **270:** 1602–1611.
30. Garber, D. W., G. Datta, M. Chaddha, M. N. Palgunachari, M. D. Garber, S. F. Doran, and G. M. Anantharamaiah. 1999. Protection against atherosclerosis in mice by synthetic class A amphipathic peptide analog of apolipoprotein A-I. *Circulation.* **100:** I538.
31. Wimley, W. C., and S. H. White. 1996. Experimentally determined hydrophobicity scale for proteins at membrane interfaces. *Nature Struc. Biol.* **3:** 842–848.
32. Morrisett, J. D., J. S. K. David, H. J. Pownall, and A. M. Gotto, Jr. 1973. Interaction of an apolipoprotein (apoLP-alanine) with phosphocholine. *Biochemistry.* **12:** 1290–1299.
33. Phillips, M. C., and K. E. Krebs. 1986. Studies of apolipoproteins at the air-water interface. *Methods Enzymol.* **128:** 387–403.
34. Ibdah, J. A., K. E. Krebs, and M. C. Phillips. 1989. The surface properties of A-I and A-II at the lipid/water interface. *Biochim. Biophys. Acta.* **1004:** 300–308.
35. Albers, J. J., C. H. Chen, and A. G. Lacko. 1986. Isolation, characterization and assay of lecithin:cholesterol acyltransferase. *Methods Enzymol.* **129:** 763–783.
36. Laemmli, U. K. 1970. Cleavage of structural proteins during the assembly of the head of bacteriophage T4. *Nature.* **227:** 680–685.
37. Navab, M., S. S. Imes, S. Y. Hama, G. P. Hough, L. A. Ross, R. W. Bork, A. J. Valente, J. A. Berliner, D. C. Drinkwater, H. Laks, and A. Fogelman. 1991. Monocyte transmigration induced by modification of low density lipoprotein in cocultures of human aortic wall cells is due to induction of monocyte chemotactic protein 1 synthesis and abolished by high density lipoprotein *J. Clin. Invest.* **88:** 2039–2046.
38. Navab, M., S. Y. Hama, B. J. Van Lenton, G. C. Fonarow, C. J. Cartinez, G. Hough, L. W. Castellini, M. L. Brennan, B. N. LaDu, A. J. Lusis, and A. M. Fogelman. 1997. Mildly oxidized LDL induces an increased apolipoprotein J/peroxanase ratio. *J. Clin. Invest.* **99:** 2005–2019.
39. Havel, R. J., H. A. Eder, and J. H. Bragdon. 1955. The distribution and chemical composition of ultracentrifugally separated lipoproteins of human serum. *J. Clin. Invest.* **43:** 1345–1353.
40. Fogelman, A. M., K. Sykes, B. J. Van Lenten, M. C. Territo, and J. A. Berliner. 1988. Modification of the Recalde method for the isolation of human monocytes. *J. Lipid Res.* **29:** 1243–1247.
41. Navab, M., L-S. Hama, B. J. Van Lenten, G. C. Fonarow, C. J. Cardinez, G. Hough, L. W. Castellani, M. L. Brennan, B. N. La Du, A. J. Lusis, and A. M. Fogelman. 1997. Mildly oxidized LDL induces an increased apolipoprotein J/paraoxonase ratio. *J. Clin. Invest.* **99:** 2005–2019.
42. Epand, R. M. 1998. Lipid polymorphism and protein-lipid interactions. *Biochim. Biophys. Acta.* **1376:** 353–368.
43. Tytler, E. M., J. P. Segrest, R. M. Epand, R. F. Epand, V. K. Mishra, Y. V. Venkatachalapathi, and G. M. Anantharamaiah. 1993. Reciprocal effects of apolipoprotein and lytic peptide analogs on membranes. *J. Biol. Chem.* **268:** 22112–22118.
44. Palgunachari, M. N., V. K. Mishra, S. Lund-Katz, M. C. Phillips, S. O. Adeyeye, S. Alluri, G. M. Anantharamaiah, and J. P. Segrest. 1996. Only the two end helixes of eight tandem amphipathic helical domains of human apo A-I have significant lipid affinity. *Arterioscler. Thromb. Vasc. Biol.* **16:** 328–338.
45. Jonas, A. 2000. Lecithin cholesterol acyltransferase. *Biochim. Biophys. Acta.* **1529:** 245–256.
46. Chung, B. H., G. M. Anantharamaiah, C. G. Brouillette, T. Nishida, and J. P. Segrest. 1985. Studies of synthetic peptide analogs of the amphipathic helix. Correlation of structure with function. *J. Biol. Chem.* **260:** 10256–10262.